Mausam, (1990), **41**, 2, 227-233

551.558.1 : 551.553.21

Impact of lateral detrainment and downdraft on the summer monsoon cloud clusters

SOMESHWAR DAS*

Centre for Atmospheric Sciences, IIT, New Delhi

सार — ग्रीष्म मानसून के विभिन्न चरणों के दौरान मेघ गुच्छों पर पार्श्व आरोहण और संरोहण अधोप्रवाह के प्रतिघात को निर्धारित करने के लिए मानावलीय कपासी समुच्चय निदर्श का प्रयोग किया गया है। यह निदर्श विभिन्न आकारों वाले मेघों की संख्या से बना हुआ है जो कि अपने जीवन चक्र के विभिन्न अवस्थाओं में होते हैं। आरोहण और संरोहण सभी स्तरों पर घटित होने पर विचार करना चाहिए। प्रत्येक कपासी मेघ कोशिका में उर्ध्ववाह और अनुवर्ती अधोप्रवाह होता है जो कि मेघ की गहराई पर आश्रित मेघ के शिखर के नीचे स्तर पर उत्पन्न होता है। इस अध्ययन के लिए मोनेक्स-79 के दौरान अरब सागर और बंगाल की खाड़ी पर बहुभुजों को बनाते हुए स्थिर जलमानों द्वारा संग्रहित ऊपरी वायु प्रेक्षणों का प्रयोग किया गया है।

ABSTRACT. A spectral cumulus ensemble model has been used to determine the impact of lateral detrainment and convective downdraft on the cloud clusters during different phases of the summer monsoon. The model consists of a population of clouds of different sizes which are in different stages of their life cycle. Entrainment and detrainment is considered to take place at all levels. Each cumulus cell has an updraft and a corresponding downdraft which originates at a level below the cloud top depending upon the depth of the cloud. Upper air observations collected from stationary ships forming polygons over the Arabian Sea and the Bay of Bengal during MONEX-79 have been used for the study.

1. Introduction

Recent studies have shown that the cumulus convection plays a major role in the onset and subsequent maintenance of the Asian summer monsoon. The latent heat released inside the cumulus clouds is a potential source of energy in the development of tropical disturbances such as the monsoon depressions. The nature of clouds and their impact on the surrounding environment vary significantly during different synoptic situations. For example, bimodal distributions of cloud base mass fluxes involving shallow and deep clouds were found over the Marshall island in the western Pacific and in the trough regions of easterly waves over the equatorial Pacific by Yanai *et al.* (1973) and Cho & Ogura (1974). On the other hand, a unimodal distribution of shallow clouds was found in the trade wind inversion zone over the western Atlantic by Nitta (1975). The heating and moistening of the surrounding environment also vary considerably. These studies provide a basis of cumulus parameterization and the results thus obtained may be used for the observational verification of a scheme.

The purpose of this study is to investigate the role of lateral detrainment and cumulus downdraft on two contrasting phases of the summer monsoon. These phases are an onset phase and a break in the monsoon phase. In the former period deep convection occurs over the warm ocean leading to the "out-burst" of the summer monsoon while, in the latter case the convection is generally suppressed causing a period of lean rainfall or break in the monsoon. Cloud cluster properties have been determined using a spectral diagnostic method. Several sensitivity experiments have been conducted to study some of the arbitrary parameters defined in the model and to determine the impact of lateral detrainment and downdraft on the summer monsoon.

2. The cumulus ensemble model

The model follows the principle of Arakawa and Schubert (1974) and Kao and Ogura (1987). It consists of a spectrum of cloud subensembles of different sizes which are in different phases of their life cycle. Clouds are classified into different types based upon their fractional rate of entrainment. Each cumulus cell consists of a convective updraft and a downdraft. Entrainment and detrainment are considered to take place at all levels in the clouds.

The large scale mean vertical mass flux $\bar{M}$ is given by:

$$\bar{M} = M_u + M_d + \widetilde{M} \tag{1}$$

where, M_u ($= \Sigma m_{ui}$) and M_d ($= \Sigma m_{di}$) are the net updraft and downdraft mass fluxes. The subscript i denotes the i^{th} cloud type. $\widetilde{M}$ is the mass flux in the sorrounding environment. The net cloud mass flux M_c is defined by :

$$M_c = M_u + M_d = \int_{\lambda=0}^{\lambda(z)} m_u(z, \lambda)\, d\lambda + \int_{\lambda=0}^{\lambda(z)} m_d(z, \lambda)\, d\lambda \tag{2}$$

*Present affiliation — National Centre for Medium Range Weather Forecasting (NCMRWF), D.S.T., New Delhi.

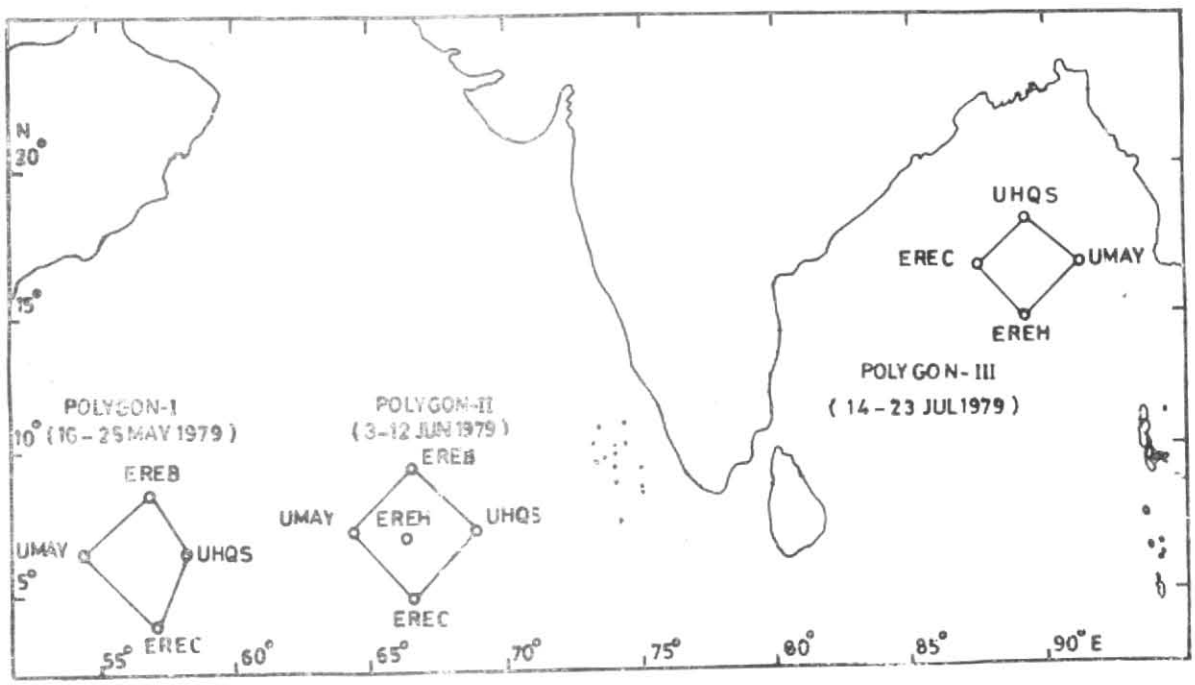

Fig. 1. Stationary positions of ships during MONEX-79

where, $m_u(z, \lambda)$ and $m_d(z, \lambda)$ are the mass flux distributions in the updrafts and the downdrafts. The double subscript (z, λ) denotes the value at the level z of a cloud type whose fractional rate of entrainment is λ.

The net fractional rate of entrainment of clouds is given by :

$$\frac{1}{m(z, \lambda)} \frac{\partial}{\partial z} m(z, \lambda) = \pm \lambda \tag{3}$$

where, $m(z, \lambda)$ is the cloud mass flux distribution in a updraft or downdraft. Negative λ stands for a downdraft. The net fractional rate of entrainment λ is equal to $\lambda_e - \lambda_d$ where, λ_e and λ_d are respectively the gross fractional entrainment and detrainment rates. It is assumed that λ_d is related to λ as :

$$\lambda_d = L_d \lambda \tag{4}$$

where, L_d is a lateral detrainment parameter. The mass fluxes of the updrafts and the downdrafts are normalised at their respective origination levels such that :

$$\eta(z, \lambda) = \frac{m(z, \lambda)}{m_R(\lambda)} \tag{5}$$

$\eta(z, \lambda)$ is called the normalised mass flux. The subscript R denotes a reference level. For the updrafts $m_R(\lambda) = m_B(\lambda)$ where, $m_B(\lambda)$ is the mass flux at the cloud base. In the downdraft $m_R(\lambda) = m_0(\lambda)$ where, $m_0(\lambda)$ is the mass flux at the downdraft origination level. It is assumed that $m_0(\lambda)$ is related to $m_B(\lambda)$ by a parameter α such that :

$$\alpha = \frac{m_0(\lambda)}{m_B(\lambda)} \tag{6}$$

The pressure at the downdraft origination level is assumed to be a function of the cloud depth and is obtained by a relation (Johnson 1976) given by :

$$P_0(\lambda) = P_B - \beta [P_B - \hat{P}(\lambda)] \tag{7}$$

where, P_B and $\hat{P}$ are respectively the pressures at the base and top of a cloud. β is called the downdraft origination level parameter.

Using the relations (3) and (5), the mass budgets for the updrafts and the downdrafts can be written as :

$$\frac{\partial}{\partial z} \eta(z, \lambda) = \pm \lambda \eta(z, \lambda) \tag{8}$$

Similarly, the heat budgets of the clouds can be written as :

$$\frac{\partial}{\partial z} [\eta(z, \lambda) h_c(z, \lambda)] = \bar{h}(z) \frac{\partial}{\partial z} \eta(z, \lambda) - L_d \lambda \eta(z, \lambda) [h_c(z, \lambda) - \bar{h}(z)] \tag{9}$$

where, h_c and $\bar{h}$ are the moist static energy of clouds and the large scale environment respectively. The subscript c refers to cloud values (updraft or downdraft). If we assume that the updrafts and downdrafts are saturated, we can obtain the relations for excess temperature and moisture of clouds over the environment (*see* Arakawa and Schubert 1974) :

$$T_c - \bar{T} \simeq \frac{1}{c_p} \frac{1}{1 + \gamma} (h_c - h^*) \tag{10a}$$

$$q_c - \bar{q}^* \simeq \frac{1}{L} \frac{\gamma}{1 + \gamma} (h_c - \bar{h}^*) \tag{10b}$$

TABLE 1

Experiments	Description	Values used	
A_1, A_2, A_3	Sensitivity of the lateral detrainment parameter (L_d)	$L_d=0$	A_1
		$L_d=0.5\left(1+\frac{P_B-P}{P_B-\hat{P}}\right)$	A_2
		$L_d=\begin{cases}-1 \text{ for } P\leq 800 \text{ mb}\\ 0 \text{ for } P>800 \text{ mb}\end{cases}$	A_3
B_1, B_2, B_3	Sensitivity of the downdraft origination level parameter (β)	$\beta=\begin{cases}0.8\\0.75\\0.5\end{cases}$	B_1 B_2 B_3
C_1, C_2, C_3	Sensitivity of the mass flux parameter (α) at the downdraft origination level	$\alpha=\begin{cases}-0.2\\-0.3\\-0.4\end{cases}$	C_1 C_2 C_3

The superscript * denotes a saturation value and

$$\gamma=L/c_p\left(\frac{\partial\bar{q}^*}{\partial T}\right)_z$$

The system of Eqns. (8), (9) and (10) are solved to obtain the cloud cluster properties λ, η, h_c, $T_c-\bar{T}$ and $q_c-\bar{q}$ using the boundary conditions :

$$h_u(\hat{z},\lambda)=\bar{h}^*(\hat{z}) \tag{11a}$$

$$h_u(z_B,\lambda)=h_M \tag{11b}$$

where, z_B and $\hat{z}$ are the heights at the base and top of a cloud. h_M is the moist static energy at the top of the mixed layer. It is assumed that the base of all clouds lie at the top of the mixed layer fixed at 950 mb. For the downdrafts it is assumed that :

$$h_d(z_0,\lambda)=\bar{h}(z_0) \tag{11c}$$

where z_0 is the height where the downdrafts originates.

The cloud base mass flux $m_B(\lambda)$ is diagnosed from the heat and moisture budget equations of the large scale environment and those of the cumulus subensembles. The final equation is written as (*see* Arakawa and Schubert 1974) :

$$Q_1-Q_2-Q_R=m_B(\lambda)\,\eta_u(p,\lambda_D)\,\frac{d\lambda_D}{dp}\left[h_u(p,\lambda_D)-\bar{h}\right]-\frac{\partial\bar{h}}{\partial p}\left\{\int_0^{\lambda_D}m_B(\lambda)\,[\eta_u(p,\lambda)+\alpha\,\eta_d(p,\lambda)]\,d\lambda\right\} \tag{12}$$

where, Q_1 and Q_2 are the apparent heat source and moisture sink. Q_R is the radiative heating rate. $\lambda_D(p)$ denotes the fractional entrainment rates of those clouds which detrain at the pressure level p.

Eqn. (12) is a volterra integral equation and is solved for $m_B(\lambda)$ by expanding it for each cloud type. The coefficients of the system of equations obtained from (12) forms a triangular matrix which can be solved easily by using an efficient algorithm.

3. Data source and method of analysis

The 6 hourly upper air observations collected from ships forming stationary polygons over the Arabian Sea and the Bay of Bengal during MONEX-79 have been used for this study. Fig. 1 shows the positions of stationary ships. During MONEX-79, three sets of observations were recorded from the stationary ships forming polygons. In each case we have used a set of data covering 10 days for this study. The first period consisted of the data from 16 to 25 May and this was considered to represent a pre-onset phase of the monsoon. The second period covered from 3 to 12 June and this was classified to represent an onset phase of the monsoon. The third period was from 14 to 23 July and this was considered to represent a phase of break in the monsoon.

Sikka and Grossman (1980) have presented a chronological weather summary of the MONEX-79. Although we have studied the cloud cluster properties in all three cases, here we shall describe the results of only the onset and the break phase. The purpose is to emphasize the difference in cloud structures between two different convective regimes.

All the data were subjected to various statistical tests to ensure internal consistency. Erroneous data were rejected and recalculated based on the observations of other ships. The horizontal derivatives such as $\nabla.V$, $\nabla\times V$, ∇T etc were obtained by a linear regression method. Divergence values were adjusted. The vertical velocity was calculated by kinematic method. The cloud ensemble model described in section 2 was discretized in a manner similar to Lord (1978) by including the lateral detrainment and convective downdraft.

4. Sensitivity experiments

This section presents the results of sensitivity experiments conducted to examine some of the arbitrary parameters defined in the formulation of the model. For example. the gross fractional rate of detrainment is asumed to be proportional to the gross fractional rate of entrainment (Eqn. 4). The constant of proportionality is called the lateral detrainment parameter L_d. Several authors (Lord 1978, Mc Bride 1981, Frank and Cohen 1987) have used different values of the parameter L_d ranging from -1.5 to 0.25. It is, therefore, quite reasonable to examine the variation in model results to different values of L_d. Another assumption made in many models is the height where the downdraft originates. The downdraft generally originates at a level where the environmental air becomes negatively buoyant due to evaporative cooling and precipitation loading. In many studies, however, it is assumed that the downdraft originates at a height above the cloud base and is a function of the total depth of the cloud. Similarly, in many studies it is assumed that the mass flux at the downdraft origination level is related to the mass flux at the cloud base through a parameter α (Eqn. 6). Frank and Cohen (1987), Kao and Ogura (1987) have used α between -0.6 and -0.3 in their studies. Since the properties of cloud clusters determined from the model depends on the values of these parameters, it is fairly important to investigate the sensitivity of results to the variation in these parameters. Table 1 summarises the sensitivity experiments conducted in this study.

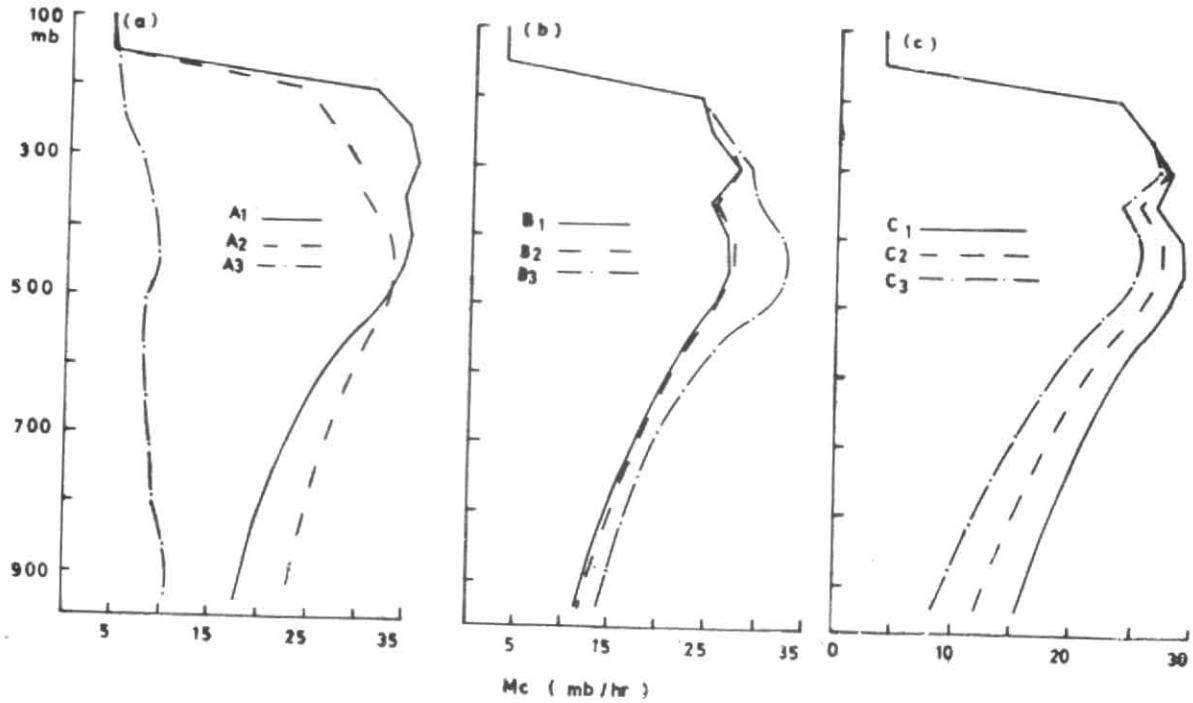

Fig. 2. Sensitivity of the total cloud mass flux M_c due to the variation in (a) lateral detrainment parameter L_d, (b) downdraft origination level parameter β and (c) mass flux parameter (α) at the downdraft origination level

Figs. 2 (a-c) show the results of sensitivity experiments. For brevity, only the results of the total cloud mass flux M_c is shown here even though the sensitivity of many other properties were also studied. Fig. 2 (a) shows that the experiments A_1 and A_2 provided maximum values of M_c between 200 & 500 mb. Experiment A_3 produced very little change in the values of M_c with height. Experiments B_1-B_2 (Fig. 2b) show that the total cloud mass flux M_c increases by lowering the height of the downdraft origination level. Results of the experiments C_1-C_3 show that M_c decreases as the ratio α is increased. This occurs because more downdraft mass flux is produced as α increases.

In the absence of actual observational measurements inside the clouds over the monsoon regime, it is difficult to assert what could be the correct values of the parameters α, β and L_d. Nevertheless, the active and weak periods of convection during the summer monsoon are to be some extent similar to the disturbed and suppressed periods of convection observed over GATE by Nitta (1977) and others. It, therefore, seems reasonable to assign $\alpha = -0.3$, $\beta = 0.75$ and L_d given by the expression A_2 (Table 1). These sets of values were found to produce better results over GATE where actual cloud measurements were available.

5. The cumulus ensemble properties

Figs. 3 (a & b) show the time averaged cloud base mass flux distribution $m_B(\lambda)$ during the onset and break phases. Each figure illustrates four different experiments which are summarised below :

Experiment No.	*Description*
i	Control run without lateral detrainment and downdraft
ii	Including lateral detrainment but without the downdraft
iii	With downdraft but without including the lateral detrainment
iv	Including both the lateral detrainment and the downdraft

Fig. 3(a) shows that there exists a unimodal distribution of deep clouds due to intense convection during the onset period. On the other hand, a bimodal distribution of both shallow and deep clouds are found during the break phase (Fig. 3b). Owing to suppressed convection in this period very few clouds have been able to develop into deeper clouds. It is evident from the figure that shallow convection dominates during this period. Comparison of the results show that the impact of lateral detrainment is to increase the cloud base mass flux while, inclusion of convective downdraft has almost no impact on the cloud base mass flux of deeper clouds. It, however, slightly reduces the cloud base mass flux of shallow clouds as is evident from Fig. 3(c). Similar results were also obtained by Nitta (1977), Johnson (1976) and McBride (1981).

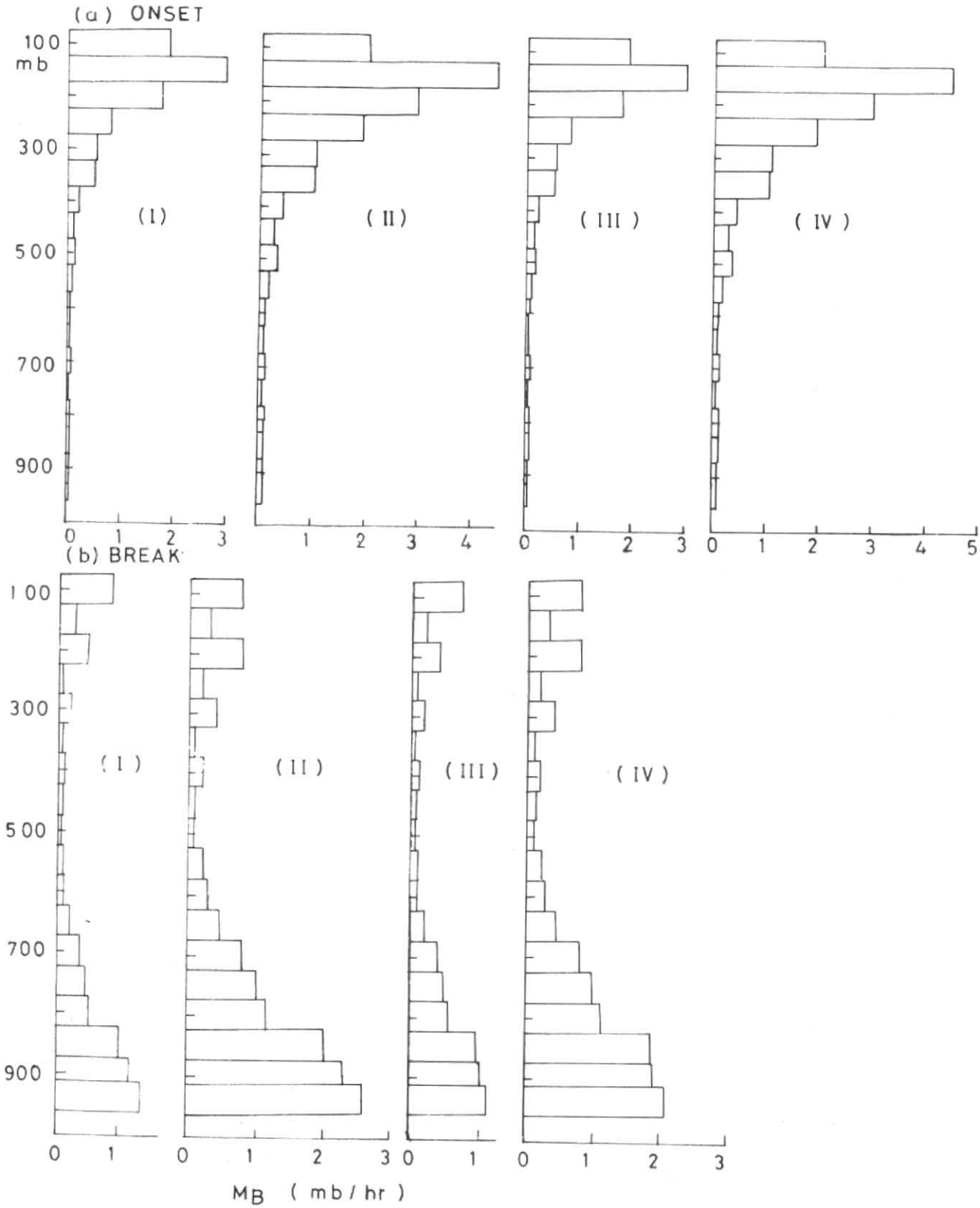

Fig. 3. Time averaged cloud base mass flux m_B (λ) of different cloud types during the (a) onset period and (b) break phase obtained by the four experiments (*i*) without including the lateral detrainment and downdraft, (*ii*) including the lateral detrainment but without the downdraft, (*iii*) without lateral detrainment but including the downdraft and (*iv*) including both the lateral detrainment and the downdraft

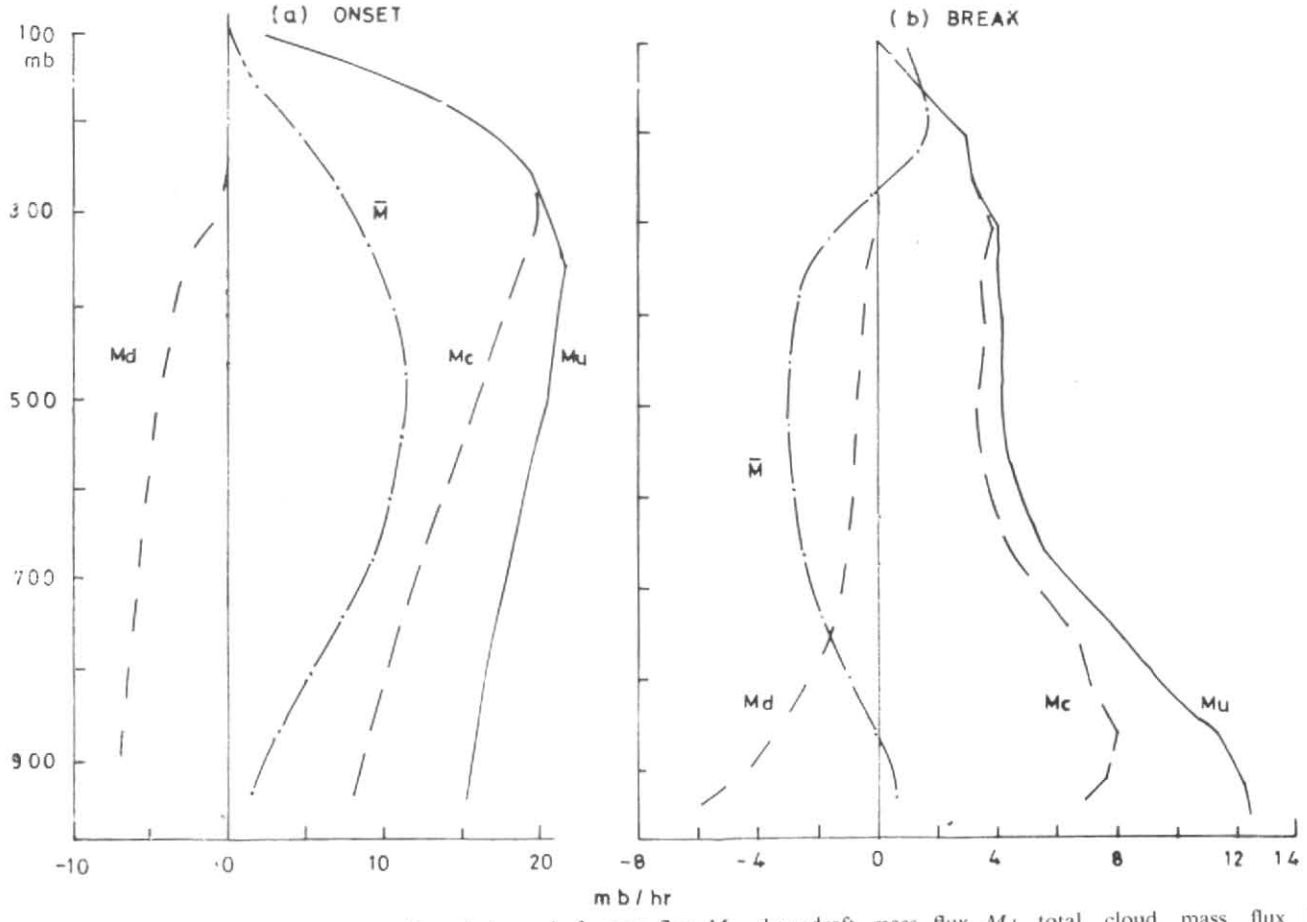

Fig. 4. Time averaged vertical profiles of the updraft mass flux M_u, downdraft mass flux M_d, total cloud mass flux M_c and the total vertical mass flux of the environment $\bar{M}$ during (a) onset and (b) break phases of the monsoon

Figs. 4(a & b) illustrate the time averaged vertical profiles of updraft mass flux M_u downdraft mass flux M_d the environmental mass flux $\bar{M}$ and the total cloud mass flux M_c during the onset and break phases. The results show that the mass flux inside the cloud updrafts is much larger than the environmental mass flux. The downdraft mass flux slowly increases downwards and has a maximum value below the cloud base. The mass flux values are stronger during the onset period. Moreover the total cloud mass flux is maximum in the upper levels in the onset phase while it is maximum in the lower troposphere during a break period. This is due to the fact that shallow convection dominates during a break in the monsoon. Fig. 4(b) also shows that there is a sinking motion in most part of the troposphere (negative $\bar{M}$) during a break in the monsoon.

Figs. 5 (a & b) illustrate the excess temperature of cloud updrafts $T_u - \bar{T}$ and the downdrafts $T_d - \bar{T}$ over the environment during the onset and break phases. Similarly Figs. 5 (c & d) show the moisture excess of the cloud updrafts $Q_u - \bar{Q}$ and the downdrafts $Q_d - \bar{Q}$ over the environment during the two phases. Results show that the cloud updrafts are about 4° to 6° C warmer than the environment during the onset phase. The downdraft temperature is generally 2° to 3° C colder than the surrounding environment except in the middle troposphere where it is slightly warmer than the environment. The downdraft temperatures are coldest below the cloud base. These results are comparable to those obtained by Nitta (1977). The results of the moisture excess (Figs. 5c, d) show that the updrafts are about 4 to 5 gm/kg moister than the surrounding environment. The maximum difference is observed in the lower troposphere. The downdrafts are less moist than the updrafts. They become drier than the environment near the cloud base.

6. Conclusion

Cloud cluster properties have been diagnosed using a spectral cumulus ensemble model during an onset and a break phase of the summer monsoon characterising two different phases of convective activity. Impact of lateral detrainment and convective downdraft has been studied.

A unimodal distribution of deep clouds is found during the onset period owing to intense convection while a biomodal distribution involving both shallow and deep clouds are found during a break phase. The total cloud mass flux M_c is maximum in the upper troposphere during the onset period due to the domination of deep clouds. M_c is maximum in the lower troposphere associated with shallow clouds during break in the monsoon. The effect of lateral detrainment is to increase the cloud mass flux. The inclusion of downdraft slightly reduces the mass flux of shallow clouds.

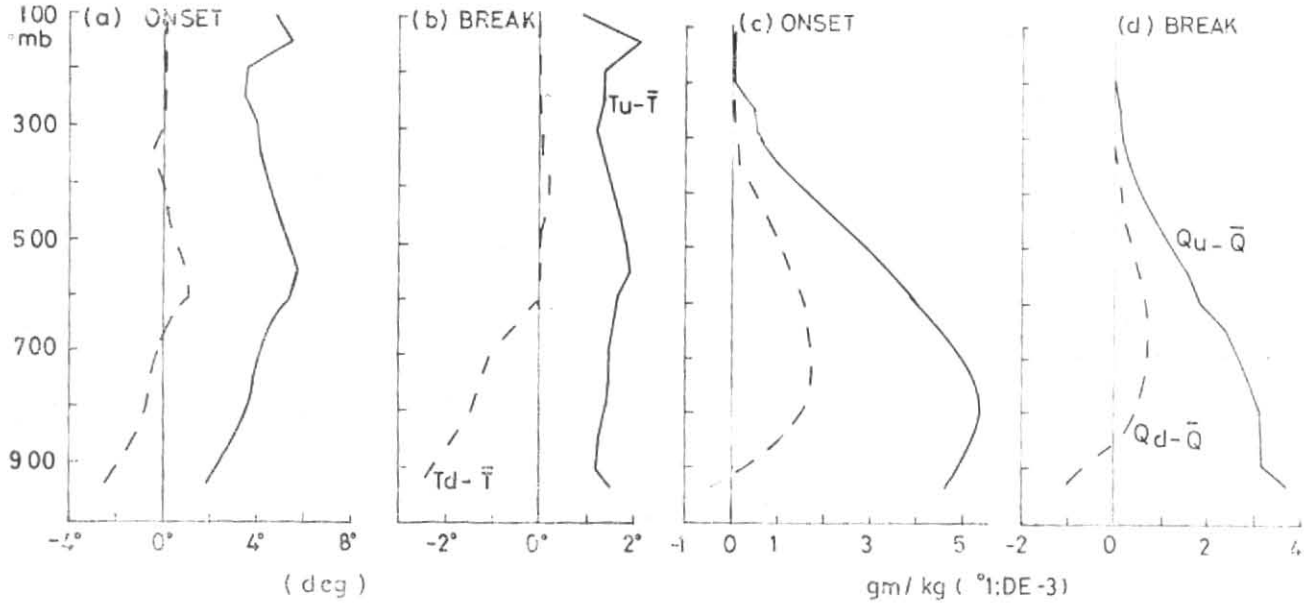

Fig. 5. Time averaged vertical profiles of excess temperature and moisture of the cloud updrafts T_u—$\bar{T}$, Q—$\bar{Q}$ and downdraft T_d—$\bar{T}$, Q_d—$\bar{Q}$ over the environment during (a & c) onset phase (b & d) break of the monsoon

The cloud updrafts are generally 4° to 6° C warmer and 4 to 5 gm/kg moister than the environment. The downdrafts are usually about 2° to 3° C colder and 1 to 2 gm/kg moister than the environment. They are drier than the environment near the cloud base.

These results indeed deserve further verification using more data sets of the monsoon regime.

Acknowledgements

The foundation of this study was led during the invaluable discussions with Prof. K. Gambo of Tokyo University while he was a visiting Professor at IIT Delhi. The author is grateful to Dr. U.C. Mohanty and Dr. O.P. Sharma for their encouragement and help provided during the course of this study. Part of the study was carried out by a financial support obtained from the Third World Academy of Sciences (TWAS). The author is grateful to Prof. M.P. Singh for kindly arranging the TWAS fellowship.

References

Arakawa, A. and Schubert, W.H., 1974, Interaction of a cumulus cloud ensemble with the large scale environment. Part I, *J. atmos. Sci.*, **31**, 674-701.

Cho, H.R. and Ogura, Y., 1974, A relationship between the cloud activity and the low level convergence as observed in Reed-Recker's composite easterly waves, *J. atmos. Sci.*, **31**, 2058-2065.

Frank, W.M. and Cohen, C., 1987, Simulation of tropical convective systems: Part I—A cumulus parameterization, *J. atmos. Sci.*, **44**, 3787-3799.

Kao, C.-Y.J. and Ogura, Y., 1987, Response of cumulus clouds to large scale forcing using the Arakawa-Schubert cumulus parameterization, *J. atmos. Sci.*, **44**, 2437-2458.

Krishnamurti, T.N., Ramanathan, Y., Ardanuy, P. and Pasch, R., 1979, Quick look "*Summer MONEX Atlas*": Part—II, The onset phase, Dept. of Meteorology, Florida State University, Tallahassee, Florida, FSU Report No. 79-5.

Lord, S.J., 1978, Development and observational verification of a cumulus cloud parameterization, Ph. D. thesis, University of California, Los Angeles, 359 pp.

Mc-Bride, J.L., 1981, An analysis of diagnostic cloud mass flux models, *J. atmos. Sci.*, **38**, 1977-1990.

Nitta, T., 1975, Observational determination of cloud mass flux distribution, *J. atmos. Sci.*, **32**, 73-91.

Nitta, T., 1977, Response of cumulus updraft and downdraft to GATE A/B-scale motion systems, *J. atmos. Sci.*, **34**, 1163-1186.

Sikka, D.R. and Bob Grossman, 1980, Summer MONEX Chronological weather summary, International MONEX Management Centre, New Delhi.

Yanai, M., Esbensen, S. and Chu, J., 1973, Determination of bulk properties of tropical cloud clusters from large scale heat and moisture budgets, *J. atmos. Sci.*, **30**, 611-627.